Title

Synchronization of the circadian clock to the environment tracked in real time.

Journal

Proceedings of the National Academy of Sciences of the United States of America, 120(13)

ISSN

0027-8424

Authors

Fang, Mingxu
Chavan, Archana G
LiWang, Andy
et al.

Publication Date

2023-03-01

DOI

10.1073/pnas.2221453120

Peer reviewed

PNAS RESEARCH ARTICLE | MICROBIOLOGY OPEN ACCESS

Synchronization of the circadian clock to the environment tracked in real time

Mingxu Fang[a], Archana G. Chavan[b], Andy LiWang[a,b,c], and Susan S. Golden[a,d,1]

Contributed by Susan S. Golden; received December 19, 2022; accepted February 8, 2023; reviewed by Luis F. Larrondo and C. Robertson McClung

The circadian system of the cyanobacterium *Synechococcus elongatus* PCC 7942 relies on a three-protein nanomachine (KaiA, KaiB, and KaiC) that undergoes an oscillatory phosphorylation cycle with a period of ~24 h. This core oscillator can be reconstituted in vitro and is used to study the molecular mechanisms of circadian timekeeping and entrainment. Previous studies showed that two key metabolic changes that occur in cells during the transition into darkness, changes in the ATP/ADP ratio and redox status of the quinone pool, are cues that entrain the circadian clock. By changing the ATP/ADP ratio or adding oxidized quinone, one can shift the phase of the phosphorylation cycle of the core oscillator in vitro. However, the in vitro oscillator cannot explain gene expression patterns because the simple mixture lacks the output components that connect the clock to genes. Recently, a high-throughput in vitro system termed the in vitro clock (IVC) that contains both the core oscillator and the output components was developed. Here, we used IVC reactions and performed massively parallel experiments to study entrainment, the synchronization of the clock with the environment, in the presence of output components. Our results indicate that the IVC better explains the in vivo clock-resetting phenotypes of wild-type and mutant strains and that the output components are deeply engaged with the core oscillator, affecting the way input signals entrain the core pacemaker. These findings blur the line between input and output pathways and support our previous demonstration that key output components are fundamental parts of the clock.

Circadian clock | Circadian phase resetting | Cyanobacteria | KaiC | Real-time monitoring

Significance

Circadian clocks are found in all kingdoms of life, where they control daily rhythmic activities from gene expression to behavior. To ensure the correct timing, daily alignment of internal clocks with the 24-h rhythm of the environment, termed entrainment, is necessary. The cyanobacterial clock has served as a model to understand how biological clocks are entrained; however, little is known about how time setting signals are transmitted from the core oscillator to gene expression. We used a high-throughput method to track the entrainment of in vitro reactions in real time and showed that some components that relay the rhythm from the core oscillator to gene expression also determine whether an environmental signal will cause a shift in the phase of the clock.

The evolution of life on Earth has been shaped by the daily fluctuation of light intensity and other environmental changes that are generated by the planet's rotation. Diverse groups of organisms have evolved biological clocks that generate circadian rhythms in physiology, metabolism, and behavior that match this 24-h time scale (1). Although the mechanisms of circadian clocks are not compositionally the same in disparate groups, they share basic functions: timekeeping, output, and entrainment (1). A clock needs a core oscillator to keep time, and components that translate this oscillation into rhythmic biological activities; additionally, the clock must stay synchronized with the environment, and reset when needed. The cyanobacterium *Synechococcus elongatus* PCC 7492 has a circadian clock that controls important physiological processes including energy metabolism and cell growth and division and is especially amenable to investigating the molecular events that underpin these capabilities (2–8).

The circadian clock of *S. elongatus* is based on a core oscillator that advances through its cycle by the interactions of the proteins KaiA, KaiB, and KaiC (9). During the day, KaiA binds to an exposed peptide of KaiC (10–13), which stimulates KaiC autophosphorylation on two residues, S431 and T432 (14, 15). The fully phosphorylated KaiC state, achieved near dusk, matures a conformation that facilitates binding of KaiB (16, 17), which acts antagonistically to damp phosphorylation by capturing KaiA (18). The result of these interactions is an ~24-h cycle of phosphorylation/dephosphorylation of the KaiC-based complex. The most striking feature of the KaiABC oscillator is that its phosphorylation/dephosphorylation cycle can be reconstituted and monitored using purified proteins in vitro (19). These in vitro oscillators (IVO) provide a unique and useful platform to probe many aspects of the clock mechanism. The Kai complex in different phosphorylation states can activate two functionally mutually antagonistic histidine protein kinases, SasA and CikA (20, 21). Both proteins act on the same DNA-binding response regulator, RpaA (22), at different times of day with SasA promoting phosphorylation of RpaA and CikA dephosphorylating RpaA, only when each is associated with the Kai complex (23). Phosphorylation of the master circadian regulator RpaA increases its DNA-binding activity; thus, rhythmic phosphorylation of KaiC eventually leads to the rhythmic expression of genes via the rhythmic phosphorylation of a transcription factor (2, 24).

Author contributions: M.F., A.L., and S.S.G. designed research; M.F. and A.G.C. performed research; M.F., A.L., and S.S.G. analyzed data; and M.F., A.L., and S.S.G. wrote the paper.

Reviewers: L.F.L., Pontifica Universidad Catolica de Chile; and C.R.M., Dartmouth College.

The authors declare no competing interest.

[1]To whom correspondence may be addressed. Email: sgolden@ucsd.edu.

This article contains supporting information online at https://www.pnas.org/lookup/suppl/doi:10.1073/pnas.2221453120/-/DCSupplemental.

Published March 20, 2023.

The cyanobacterial clock is known to be entrained by light/dark signals (25). Without a sensory photoreceptor to monitor light conditions (26), it is proposed that cyanobacteria use metabolic signals generated by photosynthesis to reset the clock. A drop in adenosine triphosphate (ATP) level occurs in vivo when the cells receive dark pulses, and in IVO reactions a change in ATP/ADP ratio was shown to change the timing of the peak of KaiC phosphorylation, shifting the phase of the oscillator (27). More recent research with an engineered *S. elongatus* strain that can use exogenous glucose showed that a change in ATP/ADP ratio caused by rhythmically feeding glucose to dark-grown cyanobacteria could indeed entrain the clock in vivo (28). Additionally, the redox state of the plastoquinone (PQ) pool is also known to entrain the cyanobacterial clock (29). Under light conditions, the quinone pool is in a relatively reduced state because photosystem II (PSII) rapidly strips electrons from water molecules to pass them to PQ (30). However, upon the onset of darkness, the quinone pool is rapidly oxidized by the cytochrome b_6f complex due to a lack of electrons from PSII, followed by a slow recovery of redox state when electrons from respiratory dehydrogenases enter the electron transport chain. It was proposed that this change in redox state of the quinone pool could be sensed by KaiA, which directly binds oxidized quinones (31, 32). Using IVO reactions, it was shown that adding oxidized quinone directly to the reactions could also shift the phosphorylation timing of KaiC (29).

In vitro reconstitution of the core oscillator has played an important role in elucidating the resetting mechanism of the cyanobacterial clock. However, the limitation of the IVO reaction is also clear: It contains only the basic timekeeping components of the clock, lacking the input-output proteins that string environmental signals, timekeeping, and gene expression together. The resetting phenotypes of mutant strains cannot be satisfactorily explained by the simple IVO reactions (20, 21). In this study, we sought to incorporate the input-output components into the IVO reactions to generate better in vitro models to study phase-shifting mechanisms of the clock. The use of a recently developed complete in vitro clock (IVC) system (33) to analyze clock-setting events demonstrated good accordance between in vitro models and in vivo results, and explained why the kinase CikA is required to elicit phase changes in vivo even though stimuli can shift the phase of the 3-protein KaiABC IVO in vitro.

Results

Shifting the Phase of In Vitro Oscillation Reactions in High-Throughput Format. Previously, fluorescence anisotropy-based assays were established to monitor the progress of the oscillation of clock proteins in vitro (33–35). This approach allowed the setup of massively parallel in vitro reactions in 384-well plates with real-time readout, facilitating large-scale experiments such as those required for the acquisition of phase response curves (PRCs) (36, 37). In this classic circadian phase-shifting assay, the magnitude of change in the phasing of a circadian activity in response to a stimulatory perturbation is probed throughout the circadian cycle, revealing the circadian rhythmicity of sensitivity. Here we first used the fluorescence from 5-carboxyfluorescein (5-FAM)-labeled KaiB as an indicator to monitor the core KaiABC oscillator (IVO) during phase shifting. In this reaction setting, the trough anisotropies of KaiB indicate free KaiB, while the peak anisotropies reflect the formation of a big KaiABC complex (35). We were able to use both oxidized quinone and adenosine diphosphate (ADP) to induce phase shifts in the oscillator in small-volume reactions in 384-well plates. As reported previously (27, 29), phase shifts were induced by adding 5 μM oxidized quinone or 1 mM ADP at different time points and reversed after 4 h by adding dithionite to reduce quinone or pyruvate kinase to convert ADP to ATP in the presence of phosphoenolpyruvate. Phase shifts were calculated by comparing circadian phases extracted from experimental reactions with those from control reactions in which dithionite or pyruvate kinase was added at the same time as oxidized quinone or ADP, respectively.

Adding oxidized quinone during the decrease arm of KaiB anisotropy caused phase shifts, with extreme cases of antiphase shifting (*SI Appendix*, Fig. S1*A*). Based on previously measured relative phases between KaiC phosphorylation and KaiB anisotropy (33), KaiC is in a low phosphorylation state in the decrease phase of KaiB anisotropy (*SI Appendix*, Fig. S1*B*). Both phase advances and phase delays were observed from KaiB anisotropy as seen in the PRC (Fig. 1*B*), in contrast to previous reports that phases of KaiC phosphorylation could be only advanced but not delayed with quinone pulses (29). Detailed analysis of KaiB anisotropy traces revealed that oxidized quinone delayed the dissociation or advanced the formation of the KaiABC nighttime complex, thus causing phase shifts (*SI Appendix*, Fig. S1*A*). We also used Cy3-labeled KaiA to monitor KaiA anisotropy during the reaction. In this assay KaiA peaks in the same phase as KaiB in a stable oscillation reaction, where peaks similarly indicate the formation of a KaiABC complex (33). Also, similarly to KaiB, KaiA showed phase shifts when quinone was added at the same time as in KaiB experiments (Fig. 1*A*). This observation, together with previous work showing that quinone can advance the KaiC phosphorylation peak (29), led to a hypothesis that upon quinone addition, quinone-bound KaiA can rapidly transit KaiC into a phosphorylated state that favors the formation of the KaiABC nighttime complex. To test this hypothesis, we set up partial clock reactions that contained labeled KaiA with KaiC phosphomimetics that represent different phosphorylation states of KaiC in the circadian cycle. We found that upon quinone addition, labeled KaiA showed an immediate increase in anisotropy only with KaiC-AA (KaiC alanine substitutions S431A and T432A), which mimics the unphosphorylated state of KaiC (Fig. 1*C*). Because KaiA is known to interact with unphosphorylated KaiC and promote its autophosphorylation activity (13), we proposed that this increase in fluorescence anisotropy indicates fast formation of a KaiAC complex that promotes KaiC's phosphorylation, which is in line with the observation that quinone phase shifts the IVO more when KaiC is less phosphorylated.

More modest phase shifts of KaiB anisotropy rhythms were observed with induction by ADP addition than with quinone (Fig. 1*B*). Although the phase shifts were small, the first KaiB anisotropy peaks after ADP addition were usually lower than for nonshift controls, which indicates a decreased formation of KaiABC complex due to dephosphorylation of KaiC (*SI Appendix*, Fig. S2).

The Effect of the Input–Output Components on the Core Oscillator during Phase Shifts. CikA was first identified in a genetic screen for resetting-deficient mutants, with its disruption abolishing normal phase resetting of the bioluminescence rhythm from a reporter gene by a pulse of darkness (20). CikA's name (**c**ircadian **i**nput **k**inase) implies its important role in transmitting environmental signals to the clock. More recent work found that including CikA in the IVO reaction can enable delays in the KaiC phosphorylation peak when quinone is added at certain circadian times (CTs), while only phase advances were observed without CikA, consistent with a role in input (38). CikA and SasA both act in output pathways where they regulate the activity of the transcription factor, and additionally affect the period of the core oscillator and

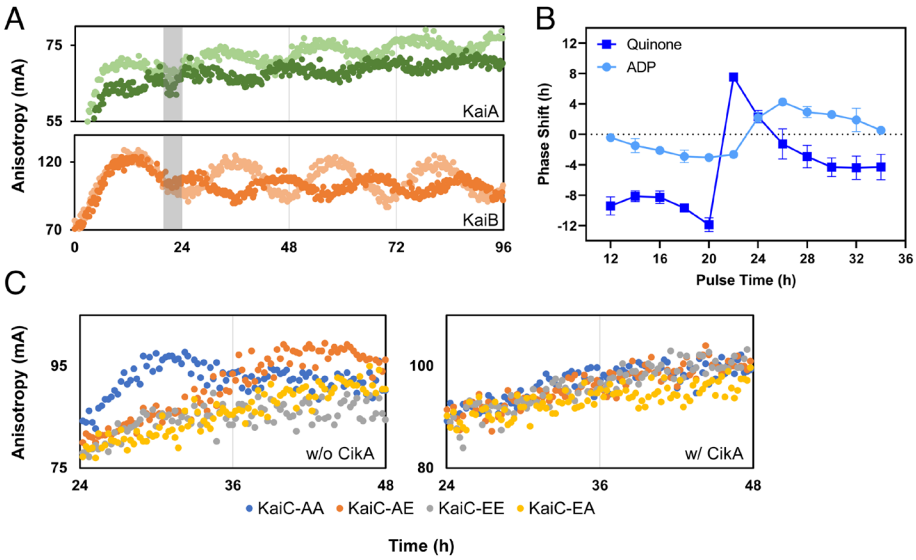

Fig. 1. Phase shifting the in vitro oscillator (IVO). (*A*) Fluorescence anisotropy rhythms of KaiA (green) and KaiB (orange) with (dark colored) or without (light colored) 4-h oxidized quinone treatment. The shaded regions indicate the duration of treatment. Each plot represents an average of 3 replicate wells. (*B*) PRCs for the IVO reactions (KaiABC only) upon oxidized quinone- or ADP-induced phase shifting. A 4-h pulse of oxidized quinone or ADP treatment was given at various times after reaction setup. The mean difference of phases between treatment and control groups is plotted. Positive values indicate phase advances and negative values indicate phase delays. Error bars show the SD (n = 2 to 4) (*C*) Fluorescence anisotropy of KaiA with KaiC phosphomimetics after quinone addition at 24 h without (w/o, *Left*) or with CikA (w/, *Right*) in partial clock reactions. Each plot represents an average of four replicates.

have features of oscillator components (23, 33, 39). These results suggest that the two kinases act beyond input-output functions in the circadian system and led us to include these proteins in clock reactions during in vitro phase shifting. To test their effects on the core oscillator, CikA and SasA were added separately or together to the basic IVO reactions and phase shifts were induced by either oxidized quinone or ADP. In wild-type *S. elongatus* cells, the rhythms from the core oscillator are transmitted to the transcription factor RpaA in the presence of both CikA and SasA; accordingly, we added CikA to KaiABC as a model for a Δ*sasA* strain, in which the generation of downstream rhythms relies solely on CikA. Similarly, a SasA-plus KaiABC reaction served as a model for a Δ*cikA* strain. By comparing the phase responses, we hoped to find an in vitro model that best explains the resetting phenotype of the wildtype and kinase-mutant strains.

In oxidized quinone-induced phase shifting, smaller phase shifts were seen from KaiB anisotropy rhythms when CikA was included in the reaction, whereas the presence of SasA did not significantly change the magnitude of phase shifts (Fig. 2*A* and *SI Appendix*, Fig. S3*A*, where plots are converted to CT). Additionally, because CikA shortens and SasA lengthens the period of oscillation, a shift in the timing of the maximum response was seen. The presence of both CikA and SasA reduced the magnitudes of phase shifts compared to those in an IVO that contained only KaiABC. By comparing PRCs for the addition of SasA vs addition of both kinases, it was determined that the absence of CikA increases the magnitude of phase shifts, which contradicts the in vivo observation that a strain lacking *cikA* cannot not properly reset upon dark pulses (20, 40). Thus, the quinone-induced phase-shifting assays do not satisfactorily explain phase shifting in vivo. The effect of CikA in buffering the clock from quinone-induced phase shifts might derive from the direct binding of quinone by the CikA pseudo-receiver (PsR) domain (41), thus lowering the concentration of free quinone in the reaction so that it can no longer trigger KaiA to interact with KaiC. Indeed, when we repeated the partial clock reactions with labeled KaiA and KaiC phosphomimetics in the presence of CikA, the increase in anisotropy seen after oxidized-quinone addition disappeared (Fig. 1*C*). Furthermore, when the amount of oxidized quinone added to induce phase shifting was increased from 5 μM to 20 μM, a significant phase shift could

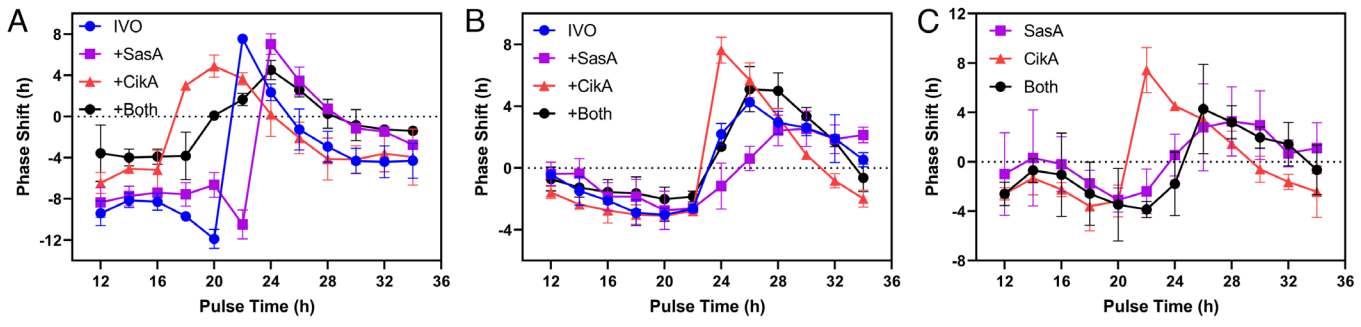

Fig. 2. Phase response curves (PRCs) upon quinone- and ADP-induced phase shifting by tracing KaiB and DNA fluorescence anisotropy rhythms. 4-h pulse of quinone (*A*) or ADP (*B* and *C*) treatment was given at various times after reaction setup. The mean difference of phases between treatment and control groups is plotted. Positive values indicate phase advances and negative values indicate phase delays. (*A* and *B*) PRCs tracing KaiB fluorescence anisotropy rhythms. Error bars show the SD (n = 2 to 4). (*C*) PRCs tracing DNA fluorescence anisotropy rhythms in in vitro clock reactions driven by either or both SasA and CikA. Error bars show the SD (n = 2 or 3).

be seen in IVO reactions with CikA (*SI Appendix*, Fig. S4*A*). Finally, when a mutant protein lacking the PsR domain, CikA-ΔPsR, was added to the reaction, a stronger phase-shifting effect could be seen (*SI Appendix*, Fig. S4*B*), which confirms the involvement of the PsR domain in buffering the IVO from quinone-induced phase shifting.

ADP-induced phase responses were also altered by the addition of the input–output proteins, but in an opposite direction (Fig. 2*B* and *SI Appendix*, Fig. S3*B*). Inclusion of CikA increased the magnitudes of phase responses whereas SasA slightly decreased them. The sensitization of IVO response to ADP by inclusion of CikA could also be seen by tracing the rhythm of KaiA (*SI Appendix*, Fig. S2). The addition of both CikA and SasA counterbalanced each protein's effect such that an intermediate magnitude of phase shift, similar to that of the IVO only reactions, was restored (Fig. 2*B*). By comparing the PRCs from conditions with both SasA and CikA vs with only SasA, we concluded that the removal of CikA reduced the magnitude of phase shifts, which is in accordance with the in vivo resetting phenotype (Fig. 2*B*). At the same time, this in vitro model system showed that the removal of SasA should sensitize the oscillation to changes in phase, predicting that a stronger magnitude of phase shift would be seen in vivo for Δ*sasA* strains.

CikA is known to interact with fold-switched KaiB (fsKaiB), a unstable conformation of KaiB that interacts with the CI domain of KaiC during the night (39). By competing with KaiA to bind fsKaiB via its PsR domain, CikA is thought to displace KaiA from the KaiABC night complex and free KaiA to stimulate KaiC phosphorylation and to promote dissociation of KaiB from dephosphorylated KaiC (33). Upon ADP addition, KaiC begins to dephosphorylate, and addition of CikA promotes displacement of KaiA from KaiB, early dissociation of KaiB from KaiC, and an early start of the phosphorylation cycle (13, 42). Thus, the PsR domain that mediates the interaction between CikA and KaiB should be important in mediating the CikA-dependent sensitivity to ADP-induced phase shifts. The histidine-kinase activity of CikA is also involved in CikA's interaction with the clock complex, because both CikA-ΔPsR, lacking the PsR domain, and CikA-H393A, which has an inactive kinase domain, disrupt KaiC's localization in vivo (43). To test this hypothesis either CikA-ΔPsR or CikA-H393A was added to the IVO reaction and partial PRCs were acquired (Fig. 3). The results showed that neither variant can cause the large phase shifts that are seen when WT CikA is in the reactions, indicating the importance of PsR-mediated interaction between CikA and the clock complex in sensitizing the oscillator's response to ADP-induced phase shifts.

SasA enhances the interaction between KaiC and KaiB through heterotropic cooperativity (33). We hypothesized that the ability of SasA to attenuate phase shifts results from this cooperativity: SasA could help to stabilize the interaction between KaiB and KaiC even upon the addition of ADP, extending the lifetime of the repressive KaiABC night complex and decreasing the effectiveness of ADP-induced phase shifts. To test whether the heterotropic cooperativity of SasA is indeed involved in SasA's ability to buffer against ADP-induced phase shifts, a SasA variant (SasA-H28A-Q94A) that has lost the ability to cooperatively recruit KaiB to KaiC (33) was used. To exaggerate the effect, a strong phase shift was induced for a KaiABC oscillator upon ADP addition in the presence of CikA. At the time of ADP addition, SasA variants were added to the reactions. Results showed that WT SasA as well as the kinase-inactive variant SasA-H161A can buffer against ADP-induced phase shifts; however, the cooperativity-incompetent SasA variant does not (Fig. 4*A*). We repeated the experiments with complete clock reactions, termed in vitro clock or IVC (detailed in the next paragraph). The IVC reactions, tracing the fluorescence anisotropy rhythm of DNA binding by RpaA (Fig. 4*B*), showed similar results to those obtained for the KaiB IVO rhythm (Fig. 4*A*).

Reporting from Other Components of the Clock during Phase Shifts. When CikA and SasA are included in reactions to generate an IVC, rhythmically phosphorylated and dephosphorylated RpaA generates rhythmic anisotropy values from a DNA probe that carries an RpaA-binding site (33). Although previously considered as an RpaA phosphatase, CikA also has kinase activity and can drive RpaA's phosphorylation cycle independently (33). To build in vitro models that better match in vivo observations, we sought to test the phase responses of IVC reactions.

We first checked the utility of oxidized quinone for shifting the phase of the IVC reactions. Unfortunately, oxidized quinone disrupted the RpaA phosphorylation cycle in IVC reactions driven by either CikA or SasA. The reduction of the quinone after 4 h

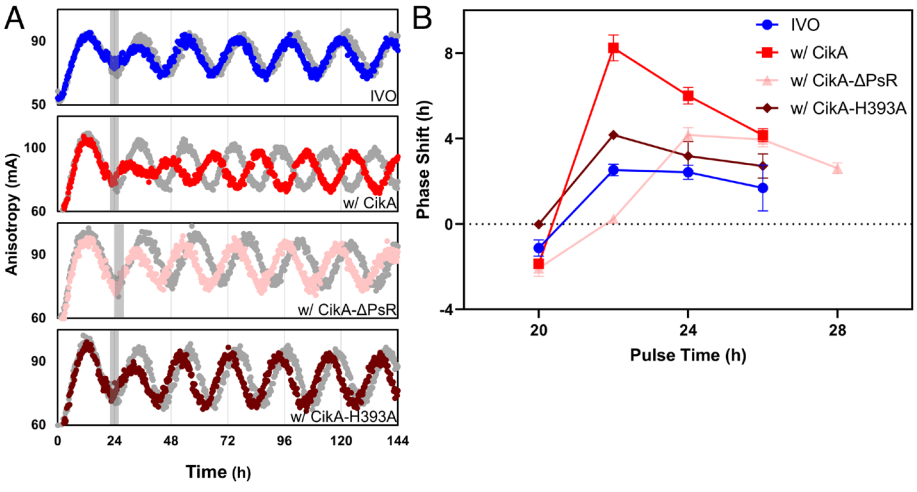

Fig. 3. CikA sensitizes the in vitro oscillator (IVO) to ADP-induced phase shifting. (*A*) Fluorescence anisotropy rhythms of KaiB upon ADP-induced phase shifting in KaiABC-only IVO or with the addition of CikA variants. Gray traces showed control rhythms while colored traces show rhythms with ADP phase shifting. These representative rhythms showed the strongest phase shifting responses the oscillation reactions can reach upon 4-h ADP treatment. The shaded regions indicate the duration of treatment. Each plot represents an average of three replicates. (*B*) Partial PRCs showing the effect of CikA variants on the IVO's response to ADP-induced phase shifting. Error bars show the SD (n = 2 or 3).

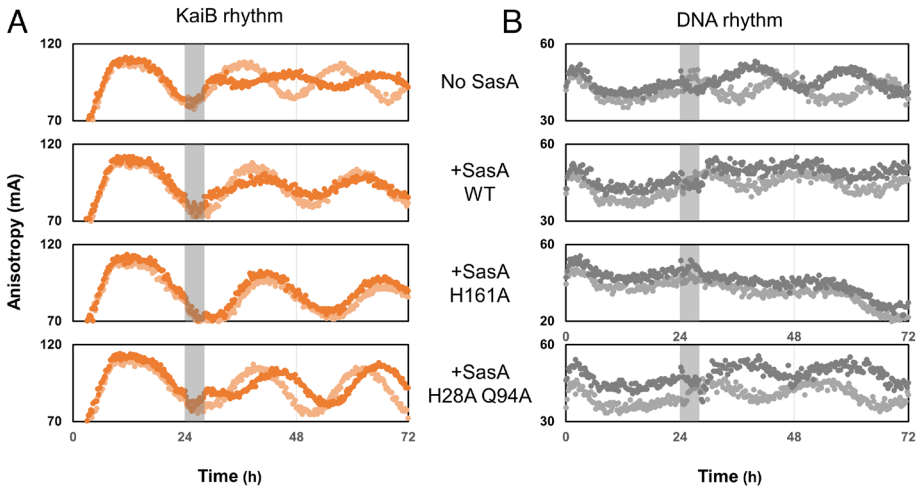

Fig. 4. SasA stabilizes CikA-dependent response to ADP-induced phase shifting. 4-h ADP treatment was given together with SasA variants at 24 h after the reaction setup. (*A*) IVO reactions tracing fluorescence anisotropy rhythms of KaiB in the presence of CikA and (*B*) IVC reactions with output driven by CikA and tracing fluorescence anisotropy rhythms of DNA were both used. The shaded regions indicate the duration of treatment. Each plot represents an average of three replicates. Darker- and lighter-shaded curves represent with and without addition of ADP, respectively.

did not restore the phosphorylation of RpaA, rendering this phase-shifting cue inappropriate for IVC reactions (*SI Appendix*, Fig. S5). Although it is possible that RpaA responds meaningfully to a redox signal, it is more likely that oxidized quinone induces an experimental artifact, because its addition lowers the fluorescence anisotropy value of the labeled DNA fragment itself.

In contrast, ADP produced phase shifts in IVC reactions with a DNA-binding readout. Because KaiB's interaction with KaiC determines the activities of both SasA and CikA (23, 33), it was not surprising that the PRCs were similar when tracing KaiB or DNA anisotropy (Fig. 2*C* and *SI Appendix*, Fig. S3*C*). As seen with the IVO, a CikA-driven clock was more sensitive to ADP-induced phase shifts and a SasA-driven clock was resistant to changes in phase. The addition of ADP affected anisotropy of the DNA probe in two ways. It affected both the core oscillator and the rate of the RpaA phosphorylation reaction. By setting up RpaA phosphorylation assays with CikA and RpaA and using DNA anisotropy as a readout, a significant drop in kinase activity was seen for CikA when ADP was added 1:1 to ATP (*SI Appendix*, Fig. S6). Similarly, 1:1 ADP to ATP also significantly decreased the KaiC-EE-induced SasA kinase activity (*SI Appendix*, Fig. S6). These results are sufficient to explain the decrease of DNA anisotropy seen upon addition of ADP. However, after the ADP pulse was reversed, the overall phase-shifting outcome reflected the state of the core oscillator rather than resulting from a kinase activity change, because the PRCs are similar between monitoring KaiB and DNA rhythms (Fig. 2).

Because we were successful in tracing three different components in IVC reactions during ADP-induced phase shifting, we sought to track the associations of each component as the clock resets. IVC reactions containing both CikA and SasA were set up with different labeled components and the response of each labeled protein was monitored during phase shifting. Although results were noisy for labeled RpaA, we acquired altered rhythms after phase shifting for all other components that could be labeled in IVC reactions (33). The changes in the components' peaking time in anisotropy showed that all components follow the core oscillator upon phase shifting to adapt to new cycles of oscillation (Fig. 5).

Verifying Resetting Phenotypes in Cyanobacterial Strains. Finally, we used reporter strains to determine whether the in vitro reactions are in good accordance with in vivo phenotypes. We knew from the ADP-induced in vitro PRCs that removal of SasA from reactions should sensitize responses to phase shifting (Fig. 2). We used the promoter of a Class 1 gene that peaks at dusk to drive the expression of a reporter luciferase gene (P*kaiBC*::*luc*) in different genetic backgrounds. Indeed, for a Δ*sasA* strain, a 4-h pulse of darkness during subjective day caused dramatic phase shifts while other strains on the same 96-well plate did not show a similar response (Fig. 6*A*). The PRCs showed the biggest response for a Δ*sasA* strain, a smaller effect for the WT strain, and the least response for Δ*cikA* strain (Fig. 6*B*). A similarly dramatic response was seen for the Δ*sasA* strain when the reporter was driven by a Class 2 promoter that peaks at dawn (P*purF*::luc), although the rhythms were too poor in either the Δ*sasA* strain or Δ*cikA* strain with the P*purF*::luc reporter to acquire a full PRC (*SI Appendix*, Fig. S7).

Discussion

This work developed an in vitro model system that satisfactorily mimics the response of the *S. elongatus* clock to environmental signals that reset the phasing of the clock. The throughput required to monitor dozens of phase changes over several cycles relied on a recent advancement in real-time monitoring of clock reactions using fluorescence anisotropy that frees the system from the labor-intensive process of tracking the KaiC phosphorylation cycle using gel-based methods. Moreover, it enables tracking changes in components other than KaiC. The IVC system allowed testing predictions that are difficult to approach in vivo. The loss of CikA is known to suppress phase changes in vivo, and we confirmed that a SasA-only IVC reaction is resistant to ADP-induced phase shifts. We also recognized an opposing function of CikA and SasA in that a CikA-only clock shifts its phase more robustly than a full clock that contains both kinases. This result encouraged us to pursue a test in vivo despite the very low residual bioluminescence of a Δ*sasA* mutant (which derives from low KaiB and KaiC levels). Indeed, the expected result was obtained (summarized in Fig. 7).

We further used this model system to better understand how CikA sensitizes while SasA stabilizes the core oscillator's response to phase shifting. Based on the observations that CikA variants that have altered ability to interact with the KaiABC complex cannot sensitize phase shifting, we proposed that CikA acts in phase shifting by displacing KaiA from fsKaiB, facilitating the

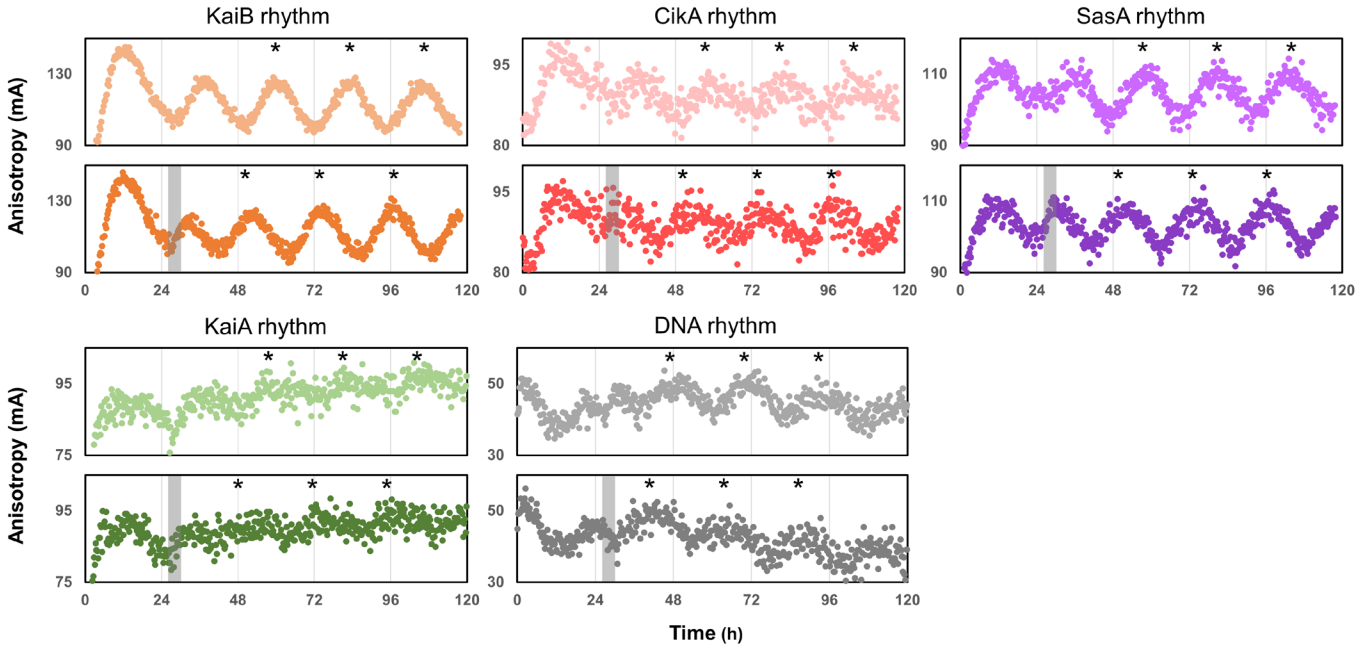

Fig. 5. Phase shifting the rhythms of different clock components. IVC reactions containing KaiA, KaiB, KaiC, CikA, SasA, RpaA and a promoter-bearing DNA fragment were subjected to a 4-h ADP-induced phase shift at 26 h after reaction setup. Different components were labeled and monitored to show advanced phases after shift (*Lower* with dark-colored plot) compared with control groups (*Upper* with light-colored plot). Stars denote the positions of the peaks.

release of KaiB from KaiC and expediting a new phosphorylation cycle. For SasA, the ability to cooperatively recruit KaiB to KaiC is crucial to buffer against phase shifting. Accordingly, we predict that SasA insulates the oscillator from ADP-induced phase shifting by enhancing the formation and extending the lifetime of the KaiABC repressive complex.

The work also provides alternative explanations to other phenotypic observations from previous work. It was proposed that the Δ*cikA* strain resets poorly because it over-accumulates glycogen, so that a dark pulse has less effect on the ATP level in vivo (40). Here, we provide evidence that CikA and SasA affect the cell's response to phase-changing signals by directly affecting the core oscillator. Purified CikA sensitizes, and while SasA counterbalances, the response of the core oscillator upon ADP-induced phase shifting in vitro. This discovery reinforces previous findings that the input–output kinases CikA and SasA are truly fundamental parts of the clock (33).

In conclusion, we have established new in vitro model systems to better understand mechanisms of the cyanobacterial circadian clock. Although the in vitro models are in good accordance with in vivo results, we recognize that cyanobacterial cells have evolved more mechanisms to fine tune the clock upon phase shifting than an in vitro model can explain. For example, it is known that the in vivo concentrations of CikA and SasA are regulated by light intensity, adding another layer of complexity after a dark pulse (44). We also noted that the in vivo phase responses of a Δ*sasA* strain are larger than the in vitro counterparts, which might be explained by the contribution of energy storage metabolism in regulating clock entrainment (40). It remains a challenge to integrate the current in vitro model with

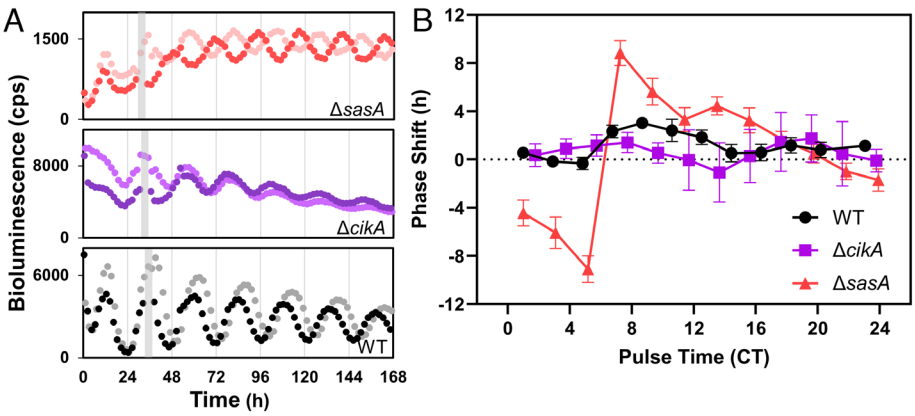

Fig. 6. In vivo phase response curves (PRCs). Rhythms of bioluminescence generated by P*kaiBC*::*luc* expression were monitored for entrained Δ*sasA* (red), Δ*cikA* (purple) and WT (black) cyanobacterial strains. (*A*) Representative rhythms showing shifted phases of Δ*sasA*, Δ*cikA* and wildtype strains that received a 4-h dark pulse at CT 7 to 8 (dark color) compared with those that remained in constant light (light color). Each plot represents an average of six biological replicates; cps, counts per second. (*B*) PRCs of the strains with 4-h dark pulse given at various circadian times. Error bars show the SD (n = 6 to 12).

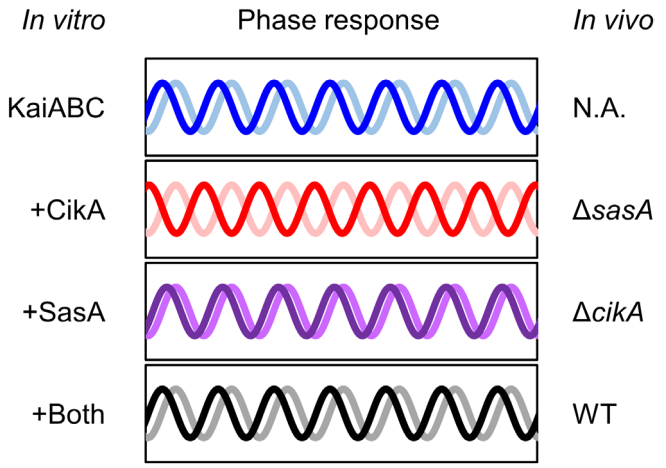

Fig. 7. In vitro clock (IVC) reactions explain well the resetting phenotypes of cyanobacterial strains. Cartoon representation of results. Darker- and lighter-shaded traces represent with and without phase-shifting stimulus, respectively. Previously, KaiABC-only IVO reactions were used to study the mechanism of entrainment of the cyanobacterial circadian clock. However, the system lacks input-output components and thus has limited ability to explain the responses of various strains upon phase shifting. In this work, we included the input-output components in the in vitro reactions and further monitored the phase shifts of the rhythmic DNA binding by the circadian master regulator RpaA. We observed that the inclusion of CikA increased the magnitudes of phase responses whereas SasA slightly decreased them. The addition of both CikA and SasA counterbalanced each protein's effect such that an intermediate magnitude of phase shift, similar to that of the IVO only reactions, was restored. Similar in vivo results were seen in the counterpart strains. Our results indicated that the responses of the IVC reactions upon ADP-induced phase shifts are in accordance with the resetting phenotypes of the respective cyanobacterial strains upon a dark pulse.

other known modulators of the clock, including LdpA, LabA, the recently discovered KidA, and the influence of protein degradation and remodeling by ClpXP (45–48). Nevertheless, the fluorescence anisotropy-based high-throughput clock reaction system has shown its value and will facilitate future research.

Materials and Methods

Strains and Plasmids. *Escherichia coli* and cyanobacterial strains were cultured, supplemented with antibiotics as needed, as previously described (49). *E. coli* strains DH5α and BL21(DE3) were used for cloning and protein overexpression, respectively. *E. coli* cells were routinely grown at 37 °C in Luria broth (LB) liquid medium with shaking or on LB plates. *S. elongatus* strains were routinely grown in liquid BG-11 medium with shaking or on BG-11 agar plates at 30 °C under continuous illumination of 100 to 150 μmol photons m^{-2} s^{-1} fluorescent cool white light.

The pET28b vector was used for overexpression and purification of all the proteins in this study. For KaiA, KaiB, KaiC, SasA and RpaA, the same 6×His-SUMO-tagged *S. elongatus* constructs were used as reported previously (33). Site-directed mutagenesis was used to generate plasmids for 6×His-SUMO-tagged SasA-H161A and SasA-H28A-Q94A. For *S. elongatus* CikA and CikA-ΔPsR (1 to 620), a sequence encoding the Strep tag (WSHPQFEKSA) was added to its N-terminal coding region and cloned into the NcoI/SacI site of pET28b. Site-directed mutagenesis was used to generate plasmids for Strep-tagged CikA-H393A.

Protein Purification and Fluorescent Labeling. For KaiA, KaiB, KaiC, SasA, and RpaA, their overexpression and purification were performed as previously reported (33) with minor modifications. A 20-mL overnight *E. coli* starter culture in LB medium was transferred to 1 L LB medium supplemented with 25 μg/mL kanamycin and grown to OD_{600}~0.5 at 37 °C before induction with 0.2 mM isopropyl β-d-1-thiogalactopyranoside overnight at 22 °C. Tris-buffered solutions were used throughout the purification steps instead of phosphate-buffered solutions as reported. For KaiA, KaiB, and KaiC, clock reaction buffer (20 mM Tris pH 8.0, 150 mM NaCl, 5 mM $MgCl_2$, 0.5 mM EDTA and 1 mM ATP) was used as elution buffer for the gel-filtration chromatography. For SasA and RpaA, a buffer containing 20 mM Tris pH 8.0, 150 mM NaCl and 5% glycerol was used as elution buffer during the gel-filtration chromatography step.

For Strep-tagged CikA variant proteins, steps before affinity purification (induction, cell lysis and clarification of cell lysate) were the same as described above except that the cells were resuspended in Strep-Tactin wash buffer (50 mM Tris pH 8.0, 150 mM NaCl, 5% glycerol and 1 mM DTT) before cell lysis. Clarified cell lysate was loaded onto a Strep-Tactin XT Superflow (IBA Lifesciences) gravity column equilibrated with Strep-Tactin wash buffer. The column was washed with Strep-Tactin wash buffer, followed by protein elution with the same buffer containing 50 mM biotin. The eluents were concentrated using spin concentrators and loaded onto a Superdex 200 column equilibrated in a buffer containing 20 mM Tris pH 8.0, 150 mM NaCl and 5% glycerol for size exclusion chromatography.

Sortase A-mediated ligation reactions were used to attach fluorophore-bearing peptides to purified proteins as previously described (33, 50). Fluorophore-labeled ssDNA and its reverse complimentary ssDNA (33) were ordered from IDT (Integrated DNA Technologies). To prepare the dsDNA fragment used in the IVC reactions, equal molar samples of the two oligonucleotides were mixed before denaturing at 95 °C for 5 min followed by slowly cooling to room temperature. KaiA and DNA fragment were labeled with Cy3; KaiB, SasA, and RpaA were labeled with 5-carboxyfluorescein (5-FAM); and CikA was labeled with 6-iodoacetamidofluorescein (6-IAF) as previously reported (33).

Monitoring In Vitro Reactions Using Fluorescence Anisotropy as Readout. The IVO reactions contain KaiA (1.2 μM), KaiB (3.5 μM) and KaiC (3.5 μM) in clock reaction buffer (20 mM Tris pH 8.0, 150 mM NaCl, 5 mM $MgCl_2$, 0.5 mM EDTA and 1 mM ATP) (19). To track the progress of the IVO, 50 nM Cy3-labeled KaiA or 5-FAM-labeled KaiB was included in the reaction while maintaining the final KaiA or KaiB concentrations unchanged. Wild-type or mutant CikA (0.7 μM) and/or SasA (0.7 μM) were added in the reactions when needed. IVC reactions contain KaiA (1.2 μM), KaiB (3.5 μM), KaiC (3.5 μM), CikA (0.7 μM) and/or SasA (0.7 μM), RpaA (2.5 μM) and a promoter-bearing Cy3-labeled dsDNA fragment (50 nM).

Reactions were set up on ice and aliquots (50 μL) of reaction master mix were pipetted into a 384-well plate before sealing with transparent film (MicroAmp™, Applied Biosystems™). Fluorescence anisotropy data were collected every 15 min in a Spark 10 M (Tecan) plate reader at 30 °C as previously reported (33). For Cy3-labeled reactions, the excitation filter was set to 520 ± 10 nm and the emission filter was set to 580 ± 10 nm. For 5-FAM- and 6-IAF-labeled reactions, 485 ± 20 nm and 535 ± 25 nm were chosen for excitation and emission filters, respectively.

To obtain PRCs, phase shifts were induced 12 h after the measurement started in the plate reader in groups of samples at 2-h interval. To shift the phase of IVO reactions with oxidized quinone, 1 μL of 250 μM Q_0 (2,3-dimethoxy-5-methyl-p-benzoquinone) was added to the 50-μL reaction mix for 4 h before the addition of 1 μL of 5 mM freshly prepared dithionite to reduce the quinone (29). Control reactions were included for each time point with quinone and dithionite added simultaneously. For all of the reactions to be phase shifted by ADP, 4 mM phosphoenolpyruvate (pH 8.0) was included in the clock reaction buffer as a part of the ATP regeneration system (27). To induce phase shifts, 1 μL of 50 mM ADP was added to the 50 μL reaction mix to lower ATP:ADP ratio to 1:1. After 4 h, 1 μL of 1 U *Bacillus stearothermophilus* pyruvate kinase (Sigma-Aldrich) was added to the reaction to convert ADP to ATP. For control reactions, ADP and pyruvate kinase were added at the same time.

Phosphorylation assays for RpaA were performed using the change in anisotropy of promoter-bearing DNA (50 nM) as an indicator (33). RpaA (2.5 μM) phosphorylation was initiated by adding CikA (0.7 μM) or SasA (0.7 μM) + KaiC-EE (3.5 μM) in clock buffer with varying ATP/ADP concentrations.

Monitoring *S. elongatus* Circadian Rhythms using Bioluminescence as Readout. Bioluminescence was monitored using firefly luciferase fusion reporters (P*kaiB::luc* and P*purF::luc*) as previously reported (33). In brief, cyanobacterial cultures were diluted and distributed onto BG-11 agar pads in 96-well plates for measuring bioluminescence with an Infinite M200 (Tecan) plate reader every 2 h. The plates were entrained for 2× 12-h light/dark cycles (80 μmol photons m^{-2} s^{-1} light) at 30 °C to synchronize phases before releasing to continuous light (30 μmol photons m^{-2} s^{-1}) during data collection. To shift the in vivo clock phase, plates were taken out of the stacker of the plate reader at different time points and covered with aluminum foil to apply dark pulses. At the end of dark pulses, plates were placed back in the stacker to continue data collection.

Generation of Phase Response Curves. Fluorescence anisotropy and bioluminescence time series data were analyzed with BioDare2 online service (https://biodare2.ed.ac.uk/) (51). Stable rhythmic data (2 h after recovery from phase shifting) with at least three cycles of oscillation were linear detrended to extract period and phase (by averaged peaks) information by the FFT NLLS method. The calculated circadian phase differences between experimental and control reactions were plotted against the phase-shifting start time in GraphPad Prism 9.

Data, Materials, and Software Availability. All study data are included in the article and/or *SI Appendix*.

ACKNOWLEDGMENT. Research reported in this publication was supported by the National Institute of General Medical Sciences of the NIH under Award Numbers R35GM118290 to S.S.G. and R35GM144110 to A.L.

Author affiliations: [a]Center for Circadian Biology, University of California, San Diego, La Jolla, CA 92093; [b]School of Natural Sciences, University of California, Merced, CA 95343; [c]Department of Chemistry & Biochemistry, University of California, Merced, CA 95343; and [d]Department of Molecular Biology, University of California, San Diego, La Jolla, CA 92093

1. D. Bell-Pedersen *et al.*, Circadian rhythms from multiple oscillators: Lessons from diverse organisms. *Nat. Rev. Genet.* **6**, 544–556 (2005).
2. J. S. Markson, J. R. Piechura, A. M. Puszynska, E. K. O'Shea, Circadian control of global gene expression by the cyanobacterial master regulator RpaA. *Cell* **155**, 1396–1408 (2013).
3. S. Diamond, D. Jun, B. E. Rubin, S. S. Golden, The circadian oscillator in *Synechococcus elongatus* controls metabolite partitioning during diurnal growth. *Proc. Natl. Acad. Sci. U.S.A.* **112**, E1916–E1925 (2015).
4. G. Dong *et al.*, Elevated ATPase activity of KaiC applies a circadian checkpoint on cell division in *Synechococcus elongatus*. *Cell* **140**, 529–539 (2010).
5. Q. Yang, B. F. Pando, G. Dong, S. S. Golden, A. Van Oudenaarden, Circadian gating of the cell cycle revealed in single cyanobacterial cells. *Science* **327**, 1522–1526 (2010).
6. Y. Liao, M. J. Rust, The circadian clock ensures successful DNA replication in cyanobacteria. *Proc. Natl. Acad. Sci. U.S.A.* **118**, e2022516118 (2021).
7. B. M. C. Martins, A. K. Tooke, P. Thomas, J. C. W. Locke, Cell size control driven by the circadian clock and environment in cyanobacteria. *Proc. Natl. Acad. Sci. U.S.A.* **115**, E11415–E11424 (2018).
8. A. M. Puszynska, E. K. O'Shea, Switching of metabolic programs in response to light availability is an essential function of the cyanobacterial circadian output pathway. *eLife* **6**, e23210 (2017).
9. J. A. Swan, S. S. Golden, A. LiWang, C. L. Partch, Structure, function, and mechanism of the core circadian clock in cyanobacteria. *J. Biol. Chem.* **293**, 5026–5034 (2018).
10. I. Vakonakis, A. C. LiWang, Structure of the C-terminal domain of the clock protein KaiA in complex with a KaiC-derived peptide: Implications for KiaC regulation. *Proc. Natl. Acad. Sci. U.S.A.* **101**, 10925–10930 (2004).
11. Y. I. Kim, G. Dong, C. W. Carruthers, S. S. Golden, A. LiWang, The day/night switch in KaiC, a central oscillator component of the circadian clock of cyanobacteria. *Proc. Natl. Acad. Sci. U.S.A.* **105**, 12825–12830 (2008).
12. M. Egli *et al.*, Loop-loop interactions regulate KaiA-stimulated KaiC phosphorylation in the cyanobacterial KaiABC circadian clock. *Biochemistry* **52**, 1208–1220 (2013).
13. R. Tseng *et al.*, Cooperative KaiA–KaiB–KaiC interactions affect KaiB/SasA competition in the circadian clock of cyanobacteria. *J. Mol. Biol.* **426**, 389–402 (2014).
14. M. J. Rust, J. S. Markson, W. S. Lane, D. S. Fisher, E. K. O'Shea, Ordered phosphorylation governs oscillation of a three-protein circadian clock. *Science* **318**, 809–812 (2007).
15. T. Nishiwaki *et al.*, A sequential program of dual phosphorylation of KaiC as a basis for circadian rhythm in cyanobacteria. *EMBO J.* **26**, 4029–4037 (2007).
16. Y. G. Chang, N. W. Kuo, R. Tseng, A. LiWang, Flexibility of the C-terminal, or CII, ring of KaiC governs the rhythm of the circadian clock of cyanobacteria. *Proc. Natl. Acad. Sci. U.S.A.* **108**, 14431–14436 (2011).
17. Y. G. Chang, R. Tseng, N. W. Kuo, A. LiWang, Rhythmic ring-ring stacking drives the circadian oscillator clockwise. *Proc. Natl. Acad. Sci. U.S.A.* **109**, 16847–16851 (2012).
18. R. Tseng *et al.*, Structural basis of the day-night transition in a bacterial circadian clock. *Science* **355**, 1174–1180 (2017).
19. M. Nakajima *et al.*, Reconstitution of circadian oscillation of cyanobacterial KaiC phosphorylation in vitro. *Science* **308**, 414–415 (2005).
20. O. Schmitz, M. Katayama, S. B. Williams, T. Kondo, S. S. Golden, CikA, a bacteriophytochrome that resets the cyanobacterial circadian clock. *Science* **289**, 765–768 (2000).
21. H. Iwasaki *et al.*, A KaiC-interacting sensory histidine kinase, SasA, necessary to sustain robust circadian oscillation in cyanobacteria. *Cell* **101**, 223–233 (2000).
22. N. Takai *et al.*, A KaiC-associating SasA-RpaA two-component regulatory system as a major circadian timing mediator in cyanobacteria. *Proc. Natl. Acad. Sci. U.S.A.* **103**, 12109–12114 (2006).
23. A. Gutu, E. K. O'Shea, Two antagonistic clock-regulated histidine kinases time the activation of circadian gene expression. *Mol. Cell* **50**, 288–294 (2013).
24. K. E. Fleming, E. K. O'Shea, An RpaA-dependent sigma factor cascade sets the timing of circadian transcriptional rhythms in *Synechococcus elongatus*. *Cell Rep.* **25**, 2937–2945.e3 (2018).
25. T. Kondo *et al.*, Circadian rhythms in prokaryotes: Luciferase as a reporter of circadian gene expression in cyanobacteria. *Proc. Natl. Acad. Sci. U.S.A.* **90**, 5672–5676 (1993).
26. S. R. Mackey, J. L. Ditty, G. Zeidner, Y. Chen, S. S. Golden, "Mechanisms for entraining the cyanobacterial circadian clock system with the environment" in *Bacterial Circadian Programs*, J. L. Ditty, S. R. Mackey, C. H. Johnson, Eds. (Springer, Berlin, Heidelberg, 2009), pp. 141–156.
27. M. J. Rust, S. S. Golden, E. K. O'Shea, Light-driven changes in energy metabolism directly entrain the cyanobacterial circadian oscillator. *Science* **331**, 220–223 (2011).
28. G. K. Pattanayak, G. Lambert, K. Bernat, M. J. Rust, Controlling the cyanobacterial clock by synthetically rewiring metabolism. *Cell Rep.* **13**, 2362–2367 (2015).
29. Y. I. Kim, D. J. Vinyard, G. M. Ananyev, G. C. Dismukes, S. S. Golden, Oxidized quinones signal onset of darkness directly to the cyanobacterial circadian oscillator. *Proc. Natl. Acad. Sci. U.S.A.* **109**, 17765–17769 (2012).
30. D. J. Lea-Smith, P. Bombelli, R. Vasudevan, C. J. Howe, Photosynthetic, respiratory and extracellular electron transport pathways in cyanobacteria. *Biochim. Biophys. Acta - Bioenerg.* **1857**, 247–255 (2016).
31. T. L. Wood *et al.*, The KaiA protein of the cyanobacterial circadian oscillator is modulated by a redox-active cofactor. *Proc. Natl. Acad. Sci. U.S.A.* **107**, 5804–5809 (2010).
32. R. Pattanayek, S. K. Sidiqi, M. Egli, Crystal structure of the redox-active cofactor dibromothymoquinone bound to circadian clock protein KaiA and structural basis for dibromothymoquinone's ability to prevent stimulation of KaiC phosphorylation by KaiA. *Biochemistry* **51**, 8050–8052 (2012).
33. A. G. Chavan *et al.*, Reconstitution of an intact clock reveals mechanisms of circadian timekeeping. *Science* **374**, eabd4453 (2021).
34. E. Leypunskiy *et al.*, The cyanobacterial circadian clock follows midday in vivo and in vitro. *eLife* **6**, e23539 (2017).
35. J. Heisler, A. Chavan, Y. G. Chang, A. Liwang, Real-time in vitro fluorescence anisotropy of the cyanobacterial circadian clock. *Methods Protoc.* **2**, 42 (2019).
36. J. Aschoff, "Response curves in circadian periodicity" in *Circadian Clocks*, J. Aschoff, Ed. (North-Holland Publishing Company, AMS, 1965), pp. 95–111.
37. C. S. Pittendrigh, "Circadian systems: Entrainment" in *Biological Rhythms*, J. Aschoff, Ed. (Springer, Boston, MA, 1981), pp. 95–124.
38. P. Kim *et al.*, CikA, an input pathway component, senses the oxidized quinone signal to generate phase delays in the cyanobacterial circadian clock. *J. Biol. Rhythms* **35**, 227–234 (2020).
39. Y. G. Chang *et al.*, A protein fold switch joins the circadian oscillator to clock output in cyanobacteria. *Science* **349**, 324–328 (2015).
40. G. K. Pattanayak, C. Phong, M. J. Rust, Rhythms in energy storage control the ability of the cyanobacterial circadian clock to reset. *Curr. Biol.* **24**, 1934–1938 (2014).
41. N. B. Ivleva, T. Gao, A. C. Liwang, S. S. Golden, Quinone sensing by the circadian input kinase of the cyanobacterial circadian clock. *Proc. Natl. Acad. Sci. U.S.A.* **103**, 17468–17473 (2006).
42. G. K. Chow *et al.*, A night-time edge site intermediate in the cyanobacterial circadian clock identified by EPR spectroscopy. *J. Am. Chem. Soc.* **144**, 184–194 (2022).
43. S. E. Cohen *et al.*, Dynamic localization of the cyanobacterial circadian clock proteins. *Curr. Biol.* **24**, 1836–1844 (2014).
44. N. B. Ivleva, M. R. Bramlett, P. A. Lindahl, S. S. Golden, LdpA: A component of the circadian clock senses redox state of the cell. *EMBO J.* **24**, 1202–1210 (2005).
45. M. Katayama, T. Kondo, J. Xiong, S. S. Golden, ldpA encodes an iron-sulfur protein involved in light-dependent modulation of the circadian period in the cyanobacterium *Synechococcus elongatus* PCC 7942. *J. Bacteriol.* **185**, 1415–1422 (2003).
46. Y. Taniguchi *et al.*, labA: A novel gene required for negative feedback regulation of the cyanobacterial circadian clock protein KaiC. *Genes Dev.* **21**, 60–70 (2007).
47. S. E. Cohen, B. M. McKnight, S. S. Golden, Roles for ClpXP in regulating the circadian clock in *Synechococcus elongatus*. *Proc. Natl. Acad. Sci. U.S.A.* **115**, E7805–E7813 (2018).
48. S. J. Kim, C. Chi, G. Pattanayak, A. R. Dinner, M. J. Rust, KidA, a multi-PAS domain protein, tunes the period of the cyanobacterial circadian oscillator. *Proc. Natl. Acad. Sci. U.S.A.* **119**, e2202426119 (2022).
49. A. Taton *et al.*, The circadian clock and darkness control natural competence in cyanobacteria. *Nat. Commun.* **11**, 1–11 (2020).
50. C. S. Theile *et al.*, Site-specific N-terminal labeling of proteins using sortase-mediated reactions. *Nat. Protoc.* **8**, 1800–1807 (2013).
51. T. Zielinski, A. M. Moore, E. Troup, K. J. Halliday, A. J. Millar, Strengths and limitations of period estimation methods for circadian data. *PLoS One* **9**, e96462 (2014).